IOP PUBLISHING JOURNAL OF PHYSICS D: APPLIED PHYSICS

J. Phys. D: Appl. Phys. **42** (2009) 085115 (9pp) doi:10.1088/0022-3727/42/8/085115

High efficiency diffractive grating coupler based on transferred silicon nanomembrane overlay on photonic waveguide

Tapas Kumar Saha and Weidong Zhou

University of Texas at Arlington, Department of Electrical Engineering, NanoFAB Center, Arlington, TX 76019-0072, USA

Received 24 January 2009, in final form 26 February 2009
Published 2 April 2009
Online at stacks.iop.org/JPhysD/42/085115

Abstract

We report here the design of a new type of high efficiency grating coupler, based on single crystalline Si nanomembrane overlay and stacking. Such high efficiency diffractive grating couplers are designed for the purpose of coupling light between single mode fibres and nanophotonic waveguides, and for the coupling between multiple photonic interconnect layers for compact three-dimensional vertical integration. Two-dimensional model simulation based on eigenmode expansion shows a diffractive power-up efficiency of 81% and a fibre coupling efficiency of 64%. With nanomembrane stacking, it is feasible to integrate the side-distributed Bragg reflector and bottom reflector, which can lead to the diffractive power-up efficiency and the fibre coupling efficiency of 97% and 73.5%, respectively. For a negatively detuned coupler, the bottom reflector is not needed, and the diffractive power-up efficiency can reach 98% over a large spectral range. The device is extremely tolerant to fabrication errors.

(Some figures in this article are in colour only in the electronic version)

1. Introduction

The recent trend of integrating the optoelectronic devices on a single chip faces a major challenge to couple light in and out of the photonic integrated circuit. Hence the idea of channelling the light from the integrated waveguide to the external environment and vice versa has attracted much attention lately. Several works have been reported in this regard based on diffraction based one-dimensional (1D) grating couplers [1–4], 45° waveguide mirrors [5], parabolic reflectors [6], etc. Aiming to couple light to and from the nanophotonic waveguide to the single mode fibre, or to build the multilayer interconnection for three-dimensional (3D) vertical integration, the diffraction based grating structure seems to be the most compact and flexible as it can be placed in any position within the photonic integrated circuit. Such a grating coupler has the disadvantage of limited fibre coupling efficiency of 37% with air cladding on top, 44% with index matching layer (IML) on top and 53% with IML on top and optimal oxide buffer thickness, as reported in [3]. In this case, the fibre coupling efficiency is calculated considering the fibre mode to be a Gaussian profile with a beam diameter of 10.4 μm. Apart from this limited coupling efficiency, the second disadvantage that such a grating coupler possesses is that the diffraction grating needs to be fabricated in the photonic waveguide through precisely controlled etching. In order to increase the coupling efficiency the simple grating structure has been adorned with a reflector grating and a bottom reflector [1], but the coupling efficiency still remains strongly dependent on the precision of the fabrication. Another common topology which is used for enhancement of the coupling efficiency is the slanted grating structure [7–9]. The slanted grating structure permits the field distribution to be centred within the waveguide, which improves the mode transition from the grating to the non-grating region and thus reduces the scattering loss at the boundary. Though the theoretical efficiency of such a structure is very high at 69.8% with only 10 grating periods as reported in [7, 8], the measured results in [9] and [10] are vastly different from the computed values since the fabrication of such a structure is

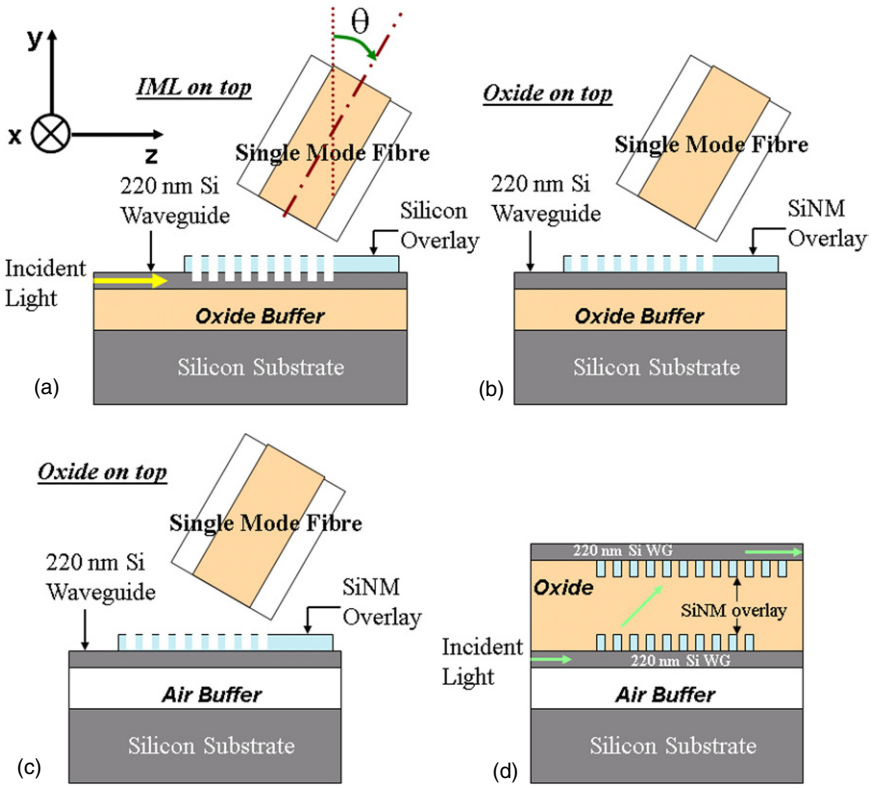

Figure 1. The schematic of diffraction based grating coupler (*a*) with deposited poly-silicon overlay and oxide buffer; (*b*) with transferred SiNM overlay and oxide buffer and (*c*) with SiNM overlay and air buffer. (*d*) Multilayer optical interconnect for high density vertical integration of optical/electrical components.

very complex and needs high precision control in both slant angle and the etching depth. To date, the highest coupling efficiency that has been reported for straight etched grating in the optical waveguide is based on the poly-silicon overlay based grating coupler structure [11, 12]. Though high coupling efficiencies of 66% theoretical and 55% experimental have been demonstrated with such a structure, precise control of etching into the silicon waveguide partially, remains necessary for its implementation [4]. Even in the most optimized structures with non-uniform grating the theoretical variation of about 5% in fibre coupling efficiency (at $\lambda = 1550$ nm) for an etch depth error of 10 nm has been reported in [4] and a variation of about 28% in fibre coupling efficiency for an etch depth error of 20 nm has been reported in [12].

In this paper we present a design to diffract light by means of a grating coupler based on single crystalline silicon nanomembrane (SiNM) overlay. The nanomembrane overlay can be patterned independently and transferred onto the photonic waveguide by means of the SiNM wet transfer and stacking process [13–15]. Such crystalline semiconductor nanomembranes offer unprecedented opportunities for unique electronic and photonic devices for vertically stacked high density photonic/electronic integration. In [12], it has been demonstrated that further improvement in fibre coupling efficiency can be obtained by using non-uniform gratings in order to better match the diffracted field profile to that of the Gaussian fibre mode. Since the rate of etching is strongly dependent on tooth width, the precise control of the etch depth in the waveguide is extremely difficult, in such non-uniform structures. The SiNM, being an etch-through structure, can find a good solution to this problem.

The paper is organized as follows. In section 2.1, the structure of the device and the details of the modified wet transfer process of the SiNM overlay on the photonic waveguide are discussed in detail. Section 2.2 throws light on the effect of air/oxide as buffer on the device structure. In section 2.3 the negatively detuned counterpart of the diffraction based grating coupler is designed, which indicates minimum loss of the optical power into the substrate. In order to increase the coupling efficiency all the more, the side-distributed Bragg reflector (DBR) and the bottom reflector have been incorporated into the grating coupler and its insensitivity to the fabrication error is analysed in section 2.4. The angle- and polarization-dependent performances are briefly discussed in section 2.5. Finally, the performances of the designed grating couplers based on SiNM overlay have been summarized in section 2.6 and the prospects and conclusions of such devices are discussed in section 3.

2. The grating coupler based on SiNM overlay

2.1. Device structure and the SiNM overlay transfer

For the sake of comparison the conventional grating coupler based on the deposited poly-silicon overlay is shown in figure 1(*a*), where the precise etching into the top silicon overlay and the bottom silicon waveguide layer is essential for maximum coupling efficiency [12]. On the other hand,

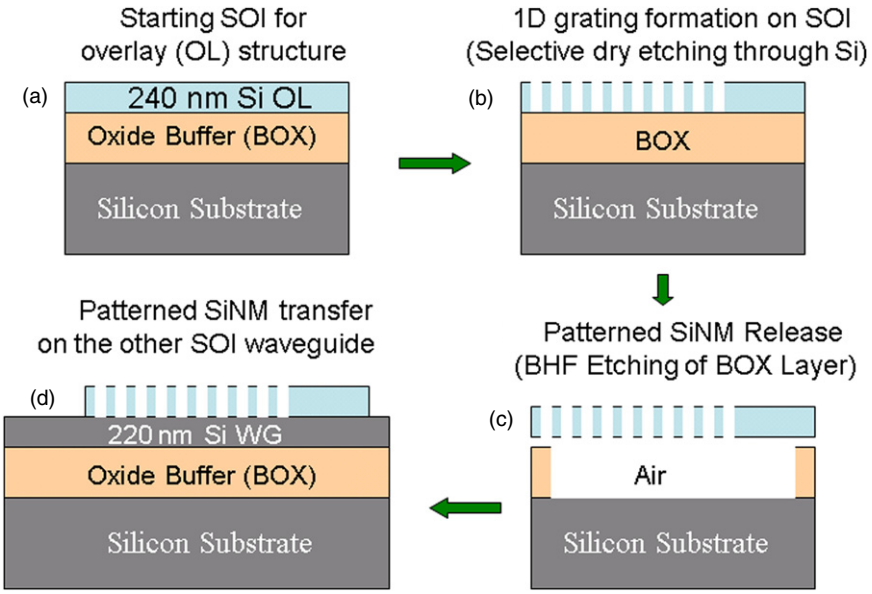

Figure 2. The modified wet transfer process for the fabrication of SiNM overlay based grating coupler on the SOI waveguide.

the proposed grating coupler based on the transferred SiNM overlay, as shown in figure 1(*b*) has a much relaxed etching depth requirement.

The wet transfer process of the SiNM overlay on the silicon on insulator (SOI) waveguide has been illustrated in figure 2. The patterning of a SiNM, its transfer and stacking on a new structure have been elaborately discussed in [15], based on the modified transfer process developed earlier by Ma and co-workers [13]. The starting material includes two SOI wafers with device layer thickness optimized independently for the waveguide layer (e.g. 220 nm) and overlay grating layer (e.g. 240 nm). The starting SOI wafer for grating overlay (figure 2(*a*)) is patterned with a complete etch-through process based on the selective dry etching of the silicon layer (figure 2(*b*)). The patterned nanomembrane (grating overlay) is subsequently released from the original hosting SOI substrate by immersing the patterned SOI sample in aqueous diluted HF solution for several hours to etch away the BOX layer selectively (figure 2(*c*)). Finally the released grating overlay layer (SiNM) is transferred on to the second SOI wafer with optical waveguide pre-defined on the Si device layer (figure 2(*d*)).

The most significant advantage of such a nanomembrane type overlay is that the performance of such a device is not sensitive to the fabrication error in the etch depth of the grating structure, since the silicon membrane is being etched through completely in the vertical direction. Another significant advantage of the SiNM overlay is that the grating coupler can be terminated by a side-DBR (also known as reflector grating, see figure 8) to enhance the coupling efficiency by preventing the transmission loss of the optical power through the SOI waveguide. This could not have been possible by a simple grating structure [1]. In [1], the authors have reported that it is necessary to design a reflector grating with the same etch depth as the coupler grating since the spacing between the two gratings plays a significant role in the device performance. On the other hand, the structure based on SiNM does not have such a constriction as no etching is actually done in the coupler section, hence a reflector grating with complete etch through the optical waveguide is feasible, which, in turn, not only ensures higher reflectance of the reflector grating but also the device remains much less sensitive to the spacing between the two gratings. This will be discussed further in more detail in the following sections. The device in figure 1(*c*) has an air buffer instead of an oxide buffer as the isolation between the optical waveguide and the silicon substrate. Such a device can be implemented by selectively etching the buffer oxide of the SOI waveguide with the buffered HF treatment as described earlier. Based on this structure, an implementation of the multilayer optical interconnects for high density vertical integration is shown in figure 1(*d*).

2.2. SiNM overlay based grating coupler performance and the effect of oxide/air as buffer layer

The device has been simulated using CAvity Modelling FRamework (CAMFR) [16, 17], which is a two-dimensional fully vectorial solver based on eigenmode expansion, with perfectly matched layer (PML) boundary conditions. The CAMFR solver has been used extensively and successfully for the design and experimental demonstration of high performance grating structures [2, 4, 11, 12]. Simulations were also carried out based on experimental results reported in [11], to ensure the accuracy of the simulation settings carried out here. The CAMFR solver is primarily used for the calculation of the diffraction efficiency, which is the ratio of the diffracted power in the superstrate (IML or oxide) to the power of the incident mode within the SOI waveguide. The transverse electric (TE) polarization, i.e. the electric field is parallel to the grating, is assumed and the target wavelength is 1550 nm. The refractive indices used in the computation were as follows: for silicon 3.476, SiO_2 (oxide) 1.444, IML 1.46 and air 1.0.

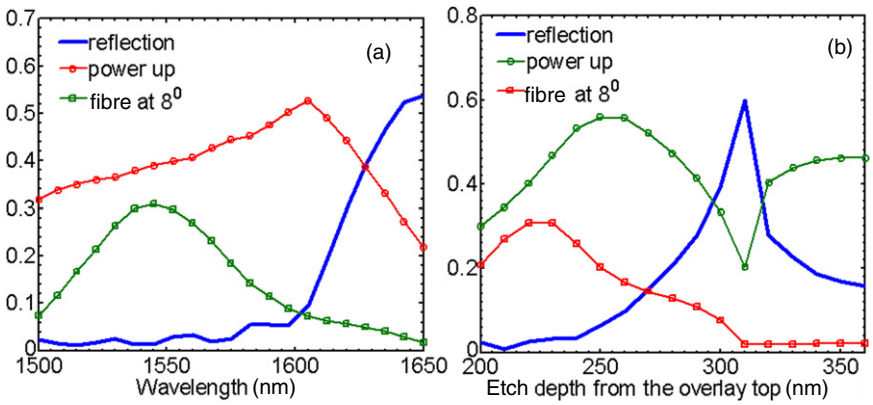

Figure 3. Simulated coupling performance for the SiNM overlay structure shown in figure 1(*b*), with IML on top and oxide buffer layer below: (*a*) wavelength dependent coupling efficiency and (*b*) the effect of etch depth from the top of the silicon overlay (SiNM) layer at $\lambda = 1550$ nm.

The device shown in figure 1(*b*) consists of a SOI waveguide structure with a 220 nm thick optical waveguide and a much larger width (i.e. 12 μm), which allows the successful 2D treatment of the device for its design analysis. As explained in [4], because of the large width of the waveguide it is a very good approximation to write the field $E_x(x, y)$ as $E_x(x)E_x(y)$. The fibre coupling efficiency is calculated [4] by using the overlap integral

$$\eta = \left| \int \vec{E} \times \vec{H}^*_{\text{fib}} \cdot \mathrm{d}\vec{S} \right|^2, \tag{1}$$

where $\vec{E}$ is the electric field vector of the diffracted light in the IML/oxide cladding and $\vec{H}_{\text{fib}}$ is the magnetic field of the fibre waveguide mode, which is also normalized in power. $\mathrm{d}\vec{S}$ lies along the surface normal of an integration pad in the air cladding which spans the complete grating coupler strength. Neglecting the smaller field components and the beam divergence in the lateral direction, equation (1) can be further simplified to [4, 18]

$$\eta = \left| \iint E(x)E(y=y_0,z)A\mathrm{e}^{-\frac{(x-x_0)^2+(z\cos\theta-z_0)^2}{\omega_0^2}} \mathrm{e}^{(\mathrm{j}n\frac{2\pi}{\lambda}z\sin\theta)}\mathrm{d}x\,\mathrm{d}z \right|^2, \tag{2}$$

where constant A represents the normalization of the Gaussian beam. For the position of the fibre y_0 is considered to be 1.5 μm as the height of the fibre above the buffer layer. θ is the angle of the fibre as shown in figure 1 and $\cos(\theta)$ is considered to be 1 for $\theta \leqslant 16^\circ$, which reduces the equation to the approximation that has been used in [4]. With this approximation the computation results agree very well with previously published results in [1–3, 12].

The waveguide is isolated from the silicon substrate by means of a buffer oxide layer of 1 μm to prevent leakage of light into the silicon substrate. The top of the grating is covered with either IML ($n = 1.46$) or silicon dioxide ($n = 1.444$) and in both the cases the simulation results vary negligibly, since the refractive index difference between the oxide and IML is only 0.016. The index matching fluid is generally applied in the case of fibre coupling to avoid the reflections at the fibre facets, whereas in the case of the high density 3D vertical integration the IML can be successfully replaced by the oxide. One important point is that equation (2) is valid for both straight cleaved or angle cleaved fibre if IML/oxide (i.e. $n = 1.46/1.44$) is used as the upper cladding layer. But if the upper cladding is considered to be air (i.e. $n = 1$), then equation (2) is only valid for straight cleaved fibres. As explained in [4], the x-dependent term in equation (2) is considered to be 0.97 for the 12 μm wide strip waveguide. The optimal value of z_0 is dependent on the grating period and the wavelength and it has been optimized in the calculation, which provides the highest coupling efficiency η for the given wavelength.

Figure 3(*a*) shows the coupling efficiency of the grating coupler based on the SiNM overlay and oxide buffer. The grating period is 560 nm with a filling factor of 50%, the SiNM overlay layer height is 220 nm, the number of the grating periods is 20 and the oxide buffer layer thickness is 1 μm. At the wavelength of 1550 nm the simulation shows that only 40% of the power is diffracted upwards and 31% is coupled to the fibre. In the actual simulation model, no fibre has been used and the coupling efficiency is calculated using the overlap integral with a Gaussian profile with a beam diameter of 10.4 μm, as done in previous papers [1–4, 12]. The fibre has been kept slightly tilted from the vertical axis at an angle of 8° to prevent second order reflection and the coupling from the fibre to the waveguide and vice versa are considered to be the same, due to reciprocity. Figure 3(*b*) provides a clearer picture of the impact etch depth on the diffraction based grating coupler. For the SiNM overlay based grating coupling structure (i.e. with an etching depth of 220 nm only on the top SiNM layer), the power-up efficiency is 40%, which is 15% lower than the over-etched conventional overlay structure, with an optimal etch depth of 250 nm (30 nm over-etching in the optical waveguide layer). This clearly signifies the fact that the etching depth into the SOI waveguide plays a very important role in increasing the efficiency of the coupling of light from the waveguide to the fibre or to the upper layer grating coupler based waveguide in the case of 3D vertical integration. However, the overlay structure can provide close to 100% power-up efficiency with the incorporation of DBRs,

due to the flexible fabrication process associated with the SiNM transfer and stacking, in addition to the advantages discussed earlier in section 2.1.

To get a further insight into the poly-Si overlay based grating coupler, the device of figure 1(*a*), which is published in [11, 12], was studied further. The diffraction properties of such a grating structure can be further modified if the oxide buffer is replaced by air. This is illustrated in figure 4. By selectively etching away the bottom oxide buffer layer, the power diffracted upwards is always higher for etch depths less than 270 nm. The grating structural parameters are kept the same as in [11, 12], i.e. the grating period of 610 nm, the Si overlay layer thickness of 150 nm and the buffer layer thickness of 2 μm. By increasing the index difference between the photonic waveguide and the isolation buffer, the field is directed much more away from the buffer and hence much more power is diffracted upwards in such a device structure.

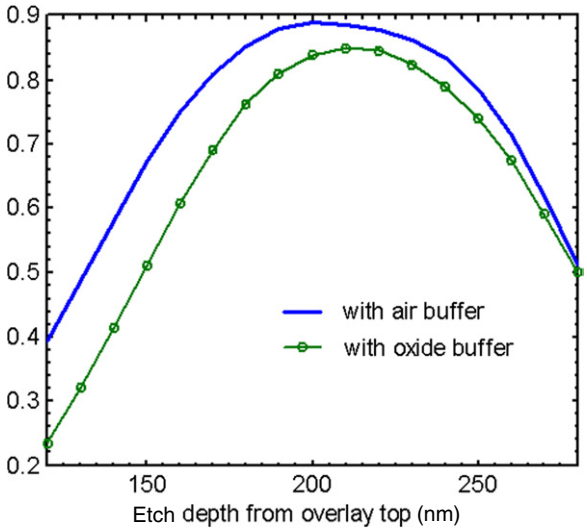

Figure 4. The variation of power diffracting upward at $\lambda = 1550$ nm for different etch depths from the overlay top, for the diffraction based grating coupler with silicon overlay. The parameters are retained the same as published in [11, 12].

So keeping this oxide effect in mind, the grating coupler based on the SiNM overlay is being designed as shown in figure 1(*c*) and the coupling result for such a structure is shown in figure 5(*a*). With a grating period of 560 nm, 50% filling factor, number of grating periods 20, overlay thickness of 220 nm, 78% of the power is diffracted up and 62% of the power is coupled into the fibre, tilted at an angle of 8° with respect to the surface-normal direction. The variation of the coupled power, for a 1550 nm wavelength, with etching depth from the overlay top is shown in figure 5(*b*). The device in this case is designed with optimum parameters with grating period 560 nm, 50% filling factor, Si overlay thickness 240 nm and air buffer thickness 1.1 μm. The air buffer thickness plays an important role since power coupled up reaches its maximum when the power, which is diffracted downwards towards the substrate, reflects from the substrate and interferes with the upward travelling wave constructively. From figure 5(*b*) it is to be noted that with the etch depth of 240 nm, i.e. when no controlled etching in the optical waveguide is required, 81% of the power is diffracted up and 64% of the power is coupled to the fibre. The maximum diffracted power is 84.3% for an etch depth of 260 nm from the overlay top, which is only a few percentage higher than the case of nanomembrane type overlay.

2.3. Positively/negatively detuned grating coupler based on SiNM overlay

In all the previously mentioned devices the light which is diffracted up takes the path in the same direction, inclined by a certain angle, in which the light was being incident in the waveguide. This is the case for the positively detuned grating coupler and, as shown in figure 1(*a*), the fibre is tilted by a positive θ angle with respect to the vertical axis. The field plot of such a device is shown in figure 6(*a*).

In contrast, when the light is diffracted up in the opposite direction with respect to the direction of incidence, the device is said to be negatively detuned, as shown in figure 6(*b*) the field propagation direction. Such a device performance based on SiNM overlay is shown in figure 7. With a grating period of 790 nm, SiNM overlay height of 240 nm, 20 periods

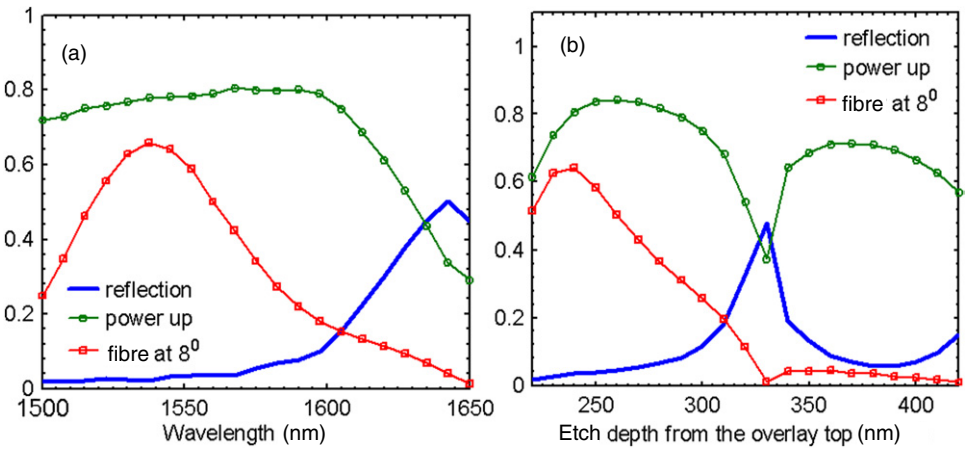

Figure 5. (*a*) Coupling efficiency of the diffraction based grating coupler with SiNM overlay, oxide on top and air buffer. (*b*) The effect of etch depth from Silicon overlay top at $\lambda = 1550$ nm.

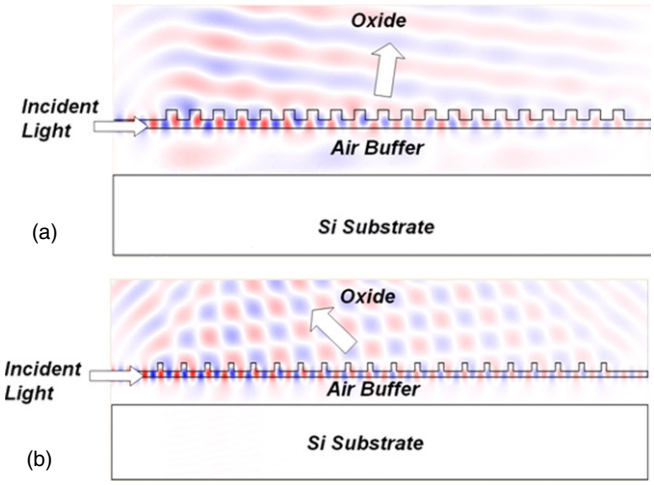

Figure 6. Field plots of the optimized grating coupler based on SiNM overlay (*a*) positively detuned and (*b*) negatively detuned.

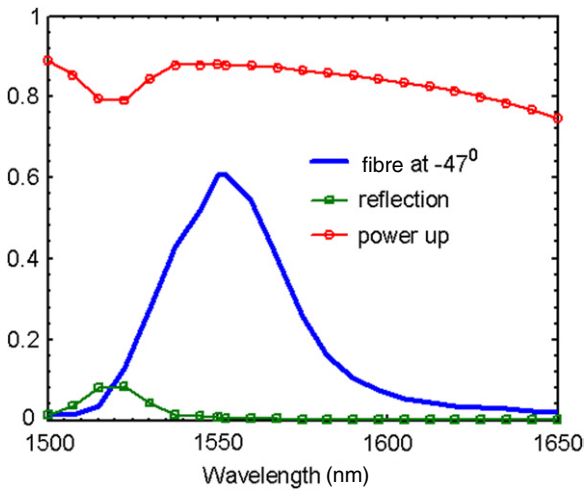

Figure 7. Coupling efficiency for a negatively detuned diffraction based grating coupler with SiNM overlay and air buffer below.

of grating, 25% filling factor and air buffer thickness of 0.8 μm the device has been optimized to diffract 88% power-up and only 2% power is lost into the substrate. One major concern for such a device is that the maximum fibre coupling efficiency is only 61%, when the fibre is held at -47° with respect to the vertical. The possible reason for this anomaly is that the field diffracted up has a large beam width and there is a large mismatch between the diffracted field profile and the Gaussian field profile of the optical fibre. In order to emphasize this point, the field plot for the negatively detuned grating coupler is shown in figure 6(*b*). Due to the principle of reciprocity, such a device can find excellent application for the realization of compact multilayer optical interconnects in the high density 3D vertical integration. This is because, considering the symmetry of the multilayer optical interconnect, as shown in figure 1(*d*), it can be inferred that the amount of power diffracted up from the bottom waveguide should be able to couple to the top waveguide completely and vice versa.

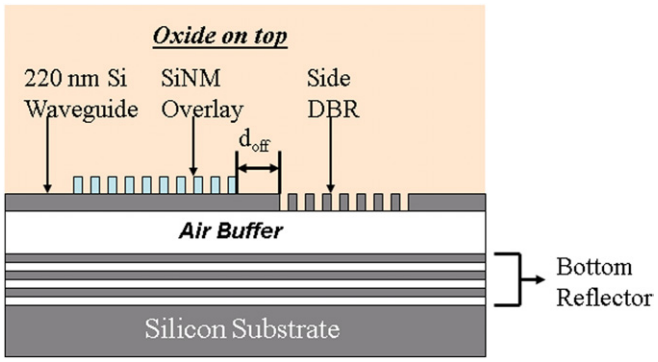

Figure 8. The grating coupler with SiNM overlay and air buffer. The coupler is terminated by a side-DBR and a bottom reflector to maximize the efficiency.

2.4. The incorporation of side-DBR and the bottom reflector

In order to further increase the coupling efficiency, the SiNM overlay based grating coupler is terminated by the side-DBR (also referred to as reflector grating in [1]) and bottom reflector. The bottom reflector can be realized by a thin layer of gold mirror [2] or DBR [1], to avoid the power loss in the silicon substrate. In this paper the bottom reflector is realized by 3 periods Si/air DBR and the side-DBR is realized by a 10 period Si/oxide DBR as shown in figure 8. Si/oxide was chosen as the side-DBR instead of Si/Air, since through CAMFR simulation it is observed that within the 220 nm optical waveguide, higher reflectivity is obtained with a Si/oxide DBR due to lesser scattering in the interface.

Two optimized SiNM based grating couplers (i.e. positively and negatively detuned), with a side-DBR and a bottom reflector are simulated for the purpose of analysis. As discussed earlier, two significant advantages of the SiNM based overlay structure are noticeable, over the previously designed structures [1]. First, the grating coupler based on the SiNM overlay is much less sensitive to the distance between the coupler grating and the side-DBR d_{off}, which is evident in figures 9(*a*) and 10(*a*). The reason is that in such a membrane type overlay based grating structure, the waveguide transmitted power through the SiNM overlay section (i.e. in plane transmission loss) is very low compared with the power which is being diffracted up. Figure 9(*a*) is the simulation result for the positively detuned grating coupler at 1550 nm wavelength, with the side-DBR and bottom reflector. The maximum occurs for d_{off} of 420 nm, where 97% of the power is diffracted up and 73.5% of the power is coupled to the fibre tilted at 8°. The minimum occurs for d_{off} of 540 nm, where 94% power is diffracted up and 71.6% of the power is coupled to the fibre. Figure 9(*b*) shows the coupling efficiency of the positively detuned coupler with respect to the wavelength. Again, the power-up efficiency varies little over a wide simulated spectral range, from 1520 to 1580 nm.

For a negatively detuned structure there is an added advantage that only 2% of the power is actually lost in the substrate and hence no bottom reflector is needed in this case. Figure 10(*a*) shows the simulation result of the negatively detuned grating coupler with 10 periods side-DBR only. In this case the maximum power coupled up is 98% for d_{off} of

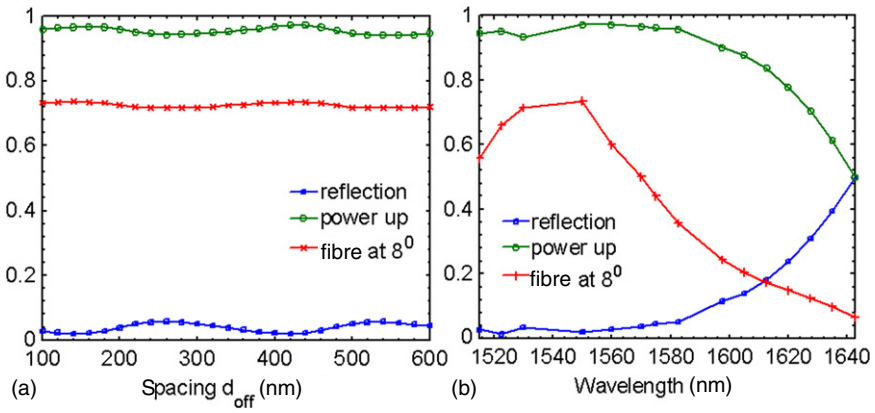

Figure 9. Performance of positively detuned SiNM overlay coupler with a side-DBR and a bottom reflector: (*a*) variation of the coupling efficiency with respect to the spacing d_{off}, the distance between the coupler grating and the side-DBR and (*b*) coupling efficiency for different wavelengths.

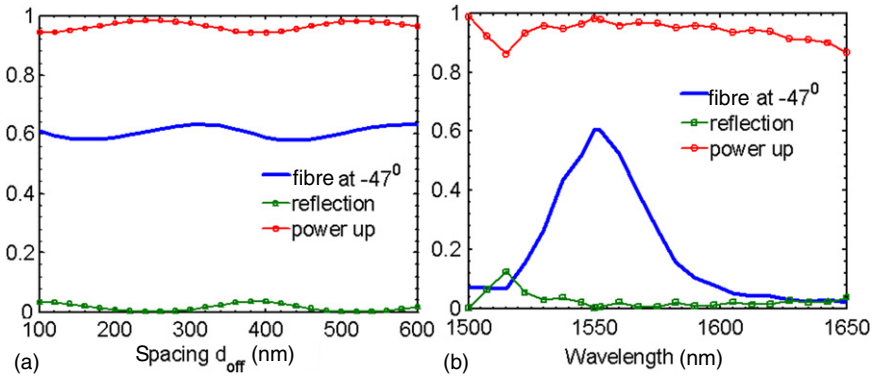

Figure 10. Performance of negatively detuned SiNM overlay coupler with a side-DBR only: (*a*) variation of the coupling efficiency with respect to the spacing d_{off} and (*b*) coupling efficiency for different wavelengths. Notice that the bottom reflector is not incorporated in this case.

240 nm, and the minimum is 94% for d_{off} of 400 nm. The maximum fibre coupled power is 63.5% for $d_{\text{off}} = 580$ nm and the minimum is 58% for $d_{\text{off}} = 440$ nm. Figure 10(*b*) shows the coupling efficiency for the negatively detuned grating coupler with respect to the wavelength. Hence, though incorporation of the side-DBR in the negatively detuned grating structure increases the power up diffraction efficiency by 10%, the fibre coupling efficiency remains practically unchanged. The possible reason for this anomaly is the large mismatch in the field profile between the reflected wave from the side-DBR and the Gaussian field profile of the optical fibre. While the positively detuned grating structure can be used for both fibre coupling and multilayer interconnection, the negative detuned structure may find immense application in the area of compact multilayer optical interconnections in photonic integrated circuits.

2.5. Salient features of diffractive grating coupler based on SiNM overlay

The fibre coupling efficiency of the designed grating coupler is dependent on the angle of the fibre which is evident from equation (2). Figure 11 shows the variation of the fibre coupling efficiency for positively and negatively detuned grating couplers based on SiNM overlay without any side-DBR and bottom reflector. For the positively detuned structure (figure 11(*a*)), the coupling efficiency is highest with 67.3% at +7° angle of fibre. For the negatively detuned counterpart (figure 11(*b*)), the coupling efficiency reaches the peak for −47° angle of fibre with an efficiency of 61%.

1D grating based devices are generally polarization sensitive, with very large polarization-dependent losses (PDLs). The devices designed here with SiNM overlay work very well for the TE polarization. In the case of transverse magnetic (TM) polarization, the optimization parameters changes vastly due to the difference in the effective index between the fundamental TE and TM modes as referred to in [19]. The fibre coupling efficiency for the TE Mode is much higher than for the TM mode because the grating coupler diffracts up the two modes at two different angles. In [4] it has been reported that for a simple grating structure with non-uniform grating, optimized for the TE mode, has a fibre coupling efficiency 21 dB lower for TM polarization. Our calculation shows that the geometry which has been optimized for the positively detuned grating coupler has resulted in a negatively detuned structure for TM polarization and vice versa, which makes it evident that the designed grating coupler will be extremely sensitive to the polarization of the light. On the other hand, polarization insensitive coupling with very small PDLs is feasible with two-dimensional grating

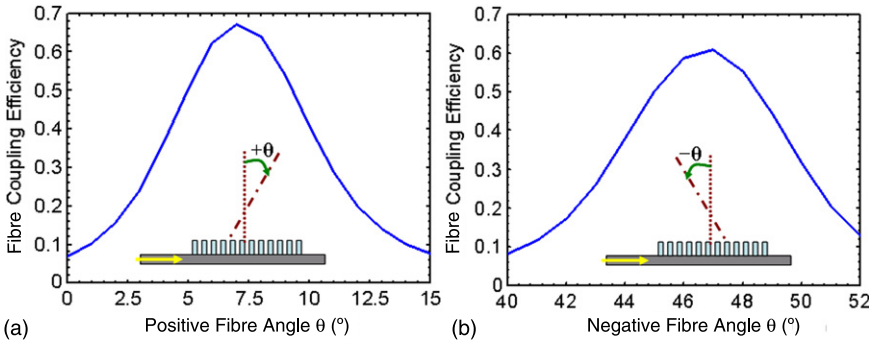

Figure 11. Variations of fibre coupling efficiencies (at wavelength $\lambda = 1550$ nm) with the coupling angles of fibre for (*a*) positively detuned and (*b*) negatively detuned diffractive grating couplers based on SiNM overlay with optimized parameters. Notice that the bottom reflector and side-DBR are not incorporated in these structures.

Table 1. Summary of the overlay based diffraction grating coupler.

Grating coupler structure	The medium on top	The buffer material	Total power up (%)	Fibre coupling (%)	Fibre angle (degree)
Poly-silicon overlay based [11, 12] (figure 1(*a*))	IML	Oxide	84	66	10
SiNM overlay based (figure 1(*b*))	IML	Oxide	40	31	8
SiNM overlay based (figure 1(*c*))	Oxide	Air	78	62	8
SiNM overlay based with optimized parameters (figure 1(*c*))	Oxide	Air	81	64	8
Negatively detuned SiNM overlay with optimized parameters (figure 1(*c*))	Oxide	Air	88	61	−47
Positively detuned SiNM overlay with optimized parameters, side-DBR and bottom reflector (figure 8)	Oxide	Air	97	73.5	8
Negatively detuned SiNM overlay based grating coupler with optimized parameters and side-DBR only (figure 8)	Oxide	Air	98	61	−47

structures or two-dimensional photonic crystal structures [15, 19, 20].

2.6. Summary

The performance of the grating couplers, designed in this paper, has been summarized in table 1. With optimized design parameters, record-high coupling efficiencies can be achieved, in the proposed SiNM structure, with 98% power-up coupling efficiency for the negatively detuned grating structure with side-DBR only. At the same time, close to 74% fibre coupling efficiency is achieved in the positively detuned SiNM overlay grating structures with side-DBR and bottom-reflectors.

3. Conclusion

In summary, a new type of diffraction based grating coupler with SiNM has been presented which does not require any kind of precisely controlled etching depth into the optical waveguide layer. The device is extremely flexible with a high coupling efficiency and promises to find immense application in fibre to nanophotonic waveguide coupling and in multilayer optical interconnections for vertically stacked high density photonic/electronic integration. Using the 2D model 78% power diffracted up and 62% power coupled to the fibre have been calculated. The negatively detuned counterpart promises to diffract 88% power up, which can be used for the design of a compact multilayer optical interconnect. Nearly 100% of the power-up efficiency has been achieved theoretically, when the side-DBR and the bottom reflector are added to the structure. The device structure is much less sensitive to the spacing between the side-DBR or reflector grating and the coupler grating than the previously reported devices.

Acknowledgments

This work was supported by the US Air Force Office of Scientific Research MURI program under Grant FA9550-08-1-0337 (Program Manager: Gernot Pomrenke). The authors

acknowledge the helpful discussions with Dr D Zhao and Dr Z Qiang.

References

[1] Taillaert D, Bogaerts W, Bienstman P, Krauss T, Van Daele P, Moerman I, Verstuyft S, De Mesel K and Baets R 2002 *IEEE J. Quantum Electron.* **38** 949–55
[2] Van Laere F, Roelkens G, Ayre M, Schrauwen J, Taillaert D, Van Thourhout D, Krauss T and Baets R 2007 *J. Lightwave Technol.* **25** 151
[3] Taillaert D, Van Laere F, Ayre M, Bogaerts W, Van Thourhout D, Bienstman P and Baets R 2006 *Japan. J. Appl. Phys* **45** 6071–7
[4] Taillaert D, Bienstman P and Baets R 2004 *Opt. Lett.* **29** 2749–51
[5] Chen R, Lin L, Choi C, Liu Y, Bihari B, Wu L, Tang S, Wickman R, Picor B and Hibb-Brenner M 2000 *Proc. IEEE* **88** 780–93
[6] Dillon T, Murakowski J, Shi S and Prather D 2008 *Opt. Lett.* **33** 896–8
[7] Wang B, Jiang J and Nordin G 2004 *Opt. Express* **12** 3313–26
[8] Wang B, Jiang J and Nordin G 2005 *IEEE Photon. Technol. Lett.* **17** 1884–6
[9] Van Laere F, Kotlyar M, Taillaert D, Van Thourhout D, Krauss T and Baets R 2007 *IEEE Photon. Technol. Lett* **19** 396
[10] Schrauwen J, Van Laere F, Van Thourhout D and Baets R 2007 *IEEE Photon. Technol. Lett* **19** 816
[11] Roelkens G, Vermeulen D, Thourhout D V, Baets R, Brision S, Lyan P, Gautier P and Fedeli J-M 2008 *Appl. Phys. Lett.* **92** 131101
[12] Roelkens G, Van Thourhout D and Baets R 2006 *Opt. Express* **14** 11622–30
[13] Yuan H C, Ma Z, Roberts M M, Savage D E and Lagally M G 2006 *J. Appl. Phys.* **100** 013708
[14] Yang H, Qiang Z, Pang H, Ma Z and Zhou W D 2008 *Electron. Lett.* **44** 858–9
[15] Qiang Z, Yang H, Chen L, Pang H, Ma Z and Zhou W D 2008 *Appl. Phys. Lett.* **93** 061106
[16] Bienstman P and Baets R 2001 *Opt. Quantum Electron.* **33** 327–41
[17] Bienstman P and Baets R 2002 *Optoelectron. IEE Proc.* **149** 161–5
[18] Vassallo C 1991 *Optical Waveguide Concepts* (Amsterdam: Elsevier)
[19] Taillaert D, Chong H, Borel P, Frandsen L, De La Rue R and Baets R 2003 *IEEE Photon. Technol. Lett.* **15** 1249–51
[20] Chen L, Qiang Z, Yang H, Pang H, Ma Z and Zhou W D 2009 *Opt. Express* Submitted